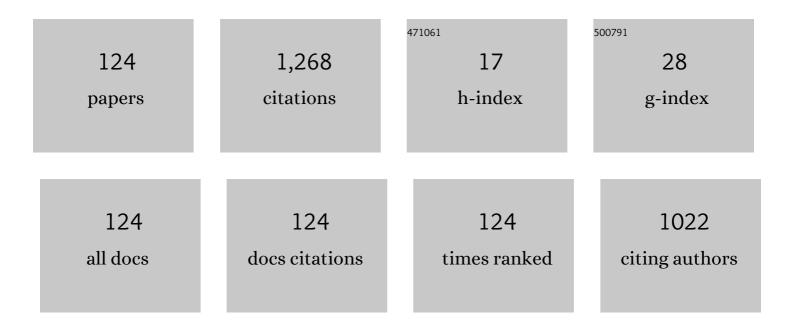
List of Publications by Year in descending order

Source: https://exaly.com/author-pdf/888494/publications.pdf Version: 2024-02-01



#	Article	IF	CITATIONS
1	A 54.4–90 GHz Low-Noise Amplifier in 65-nm CMOS. IEEE Journal of Solid-State Circuits, 2017, 52, 2892-2904.	3.5	91
2	A Scalable Large-Signal Multiharmonic Model of AlGaN/GaN HEMTs and Its Application in C-Band High Power Amplifier MMIC. IEEE Transactions on Microwave Theory and Techniques, 2017, 65, 2836-2846.	2.9	80
3	Analysis and Design of Ultra-Wideband mm-Wave Injection-Locked Frequency Dividers Using Transformer-Based High-Order Resonators. IEEE Journal of Solid-State Circuits, 2018, 53, 2177-2189.	3.5	55
4	A 20 ~ 43 GHz VGA with 21.5 dB Gain Tuning Range and Low Phase Variation for 5G Communications in 65-nm CMOS. , 2019, , .		46
5	Analysis and Equivalent-Circuit Model for CMOS On-Chip Multiple Coupled Inductors in the Millimeter-Wave Region. IEEE Transactions on Electron Devices, 2015, 62, 3957-3964.	1.6	40
6	Triple bandâ€notched UWB monopole antenna on ultraâ€ŧhin liquid crystal polymer based on ESCSRR. Electronics Letters, 2017, 53, 57-58.	0.5	38
7	A Broadband and Equivalent-Circuit Model for Millimeter-Wave On-Chip M:N Six-Port Transformers and Baluns. IEEE Transactions on Microwave Theory and Techniques, 2015, 63, 3109-3121.	2.9	35
8	Temperature-Dependent Access Resistances in Large-Signal Modeling of Millimeter-Wave AlGaN/GaN HEMTs. IEEE Transactions on Microwave Theory and Techniques, 2017, 65, 2271-2278.	2.9	34
9	An Injection-Current-Boosting Locking-Range Enhancement Technique for Ultra-Wideband mm-Wave Injection-Locked Frequency Triplers. IEEE Transactions on Microwave Theory and Techniques, 2019, 67, 3174-3186.	2.9	31
10	Analysis and Design of Inductorless Wideband Low-Noise Amplifier With Noise Cancellation Technique. IEEE Access, 2017, 5, 9389-9397.	2.6	30
11	A 62-90 GHz High Linearity and Low Noise CMOS Mixer Using Transformer-Coupling Cascode Topology. IEEE Access, 2018, 6, 19338-19344.	2.6	27
12	A CMOS K-Band 6-bit Attenuator With Low Phase Imbalance for Phased Array Applications. IEEE Access, 2017, 5, 19657-19661.	2.6	25
13	A 256-QAM 39 GHz Dual-Channel Transceiver Chipset with LTCC Package for 5G Communication in 65 nm CMOS. , 2018, , .		25
14	An On-Chip Frequency-Reconfigurable Antenna For Q-Band Broadband Applications. IEEE Antennas and Wireless Propagation Letters, 2017, 16, 2232-2235.	2.4	21
15	A Ku band 4-Element phased array transceiver in 180 nm CMOS. , 2017, , .		20
16	High-Temperature-Annealed Flexible Carbon Nanotube Network Transistors for High-Frequency Wearable Wireless Electronics. ACS Applied Materials & Interfaces, 2020, 12, 26145-26152.	4.0	20
17	Microwave transmission properties of chemical vapor deposition graphene. Applied Physics Letters, 2012, 101, 053110.	1.5	19
18	A 60-GHz Variable Gain Phase Shifter With 14.8-dB Gain Tuning Range and 6-Bit Phase Resolution Across â^'25 °C–110 °C. IEEE Transactions on Microwave Theory and Techniques, 2021, 69, 2371-2385.	2.9	19

#	Article	IF	CITATIONS
19	A 21-to-41-GHz High-Gain Low Noise Amplifier With Triple-Coupled Technique for Multiband Wireless Applications. IEEE Transactions on Circuits and Systems II: Express Briefs, 2021, 68, 1857-1861.	2.2	19
20	A 37–40-GHz Low-Phase-Imbalance CMOS Attenuator With Tail-Capacitor Compensation Technique. IEEE Transactions on Circuits and Systems I: Regular Papers, 2020, 67, 3400-3409.	3.5	18
21	Xâ€band flexible bandpass filter based on ultraâ€ŧhin liquid crystal polymer substrate. Electronics Letters, 2015, 51, 345-347.	0.5	17
22	An Improved Ultrawideband Open-Short De-Embedding Method Applied up to 220 GHz. IEEE Transactions on Components, Packaging and Manufacturing Technology, 2018, 8, 269-276.	1.4	17
23	An Ultralow Phase Noise Eight-Core Fundamental 62-to-67-GHz VCO in 65-nm CMOS. IEEE Microwave and Wireless Components Letters, 2019, 29, 125-127.	2.0	17
24	A 19.5% Efficiency 51–73-GHz High-Output Power Frequency Doubler in 65-nm CMOS. IEEE Microwave and Wireless Components Letters, 2019, 29, 818-821.	2.0	17
25	A Compact Ka-Band Active Integrated Antenna With a GaAs Amplifier in a Ceramic Package. IEEE Antennas and Wireless Propagation Letters, 2017, 16, 2416-2419.	2.4	15
26	A 51.5 - 64.5 GHz Active Phase Shifter Using Linear Phase Control Technique With 1.4° Phase resolution in 65-nm CMOS. , 2019, , .		15
27	Analytical Gate Capacitance Models for Large-Signal Compact Model of AlGaN/GaN HEMTs. IEEE Transactions on Electron Devices, 2019, 66, 357-363.	1.6	15
28	A 21.7-to-41.7-GHz Injection-Locked LO Generation With a Narrowband Low-Frequency Input for Multiband 5G Communications. IEEE Transactions on Microwave Theory and Techniques, 2020, 68, 170-183.	2.9	15
29	A Large-Signal Statistical Model and Yield Estimation of GaN HEMTs Based on Response Surface Methodology. IEEE Microwave and Wireless Components Letters, 2016, 26, 690-692.	2.0	14
30	A Hybrid Integrated High-Gain Antenna With an On-Chip Radiator Backed by Off-Chip Ground for System-on-Chip Applications. IEEE Transactions on Components, Packaging and Manufacturing Technology, 2017, 7, 114-122.	1.4	13
31	Flexible Graphene Field-Effect Transistors With Extrinsic <inline-formula> <tex-math notation="LaTeX">\${f}_{{{mathrm{max}}}\$ </tex-math </inline-formula> of 28 GHz. IEEE Electron Device Letters, 2018, 39, 1944-1947.	2.2	13
32	Characterization of CVD graphene permittivity and conductivity in micro-/millimeter wave frequency range. AIP Advances, 2016, 6, 095014.	0.6	12
33	A 27.5–43.5 GHz high linearity up-conversion CMOS mixer for 5G communication. , 2017, , .		12
34	A <i>K</i> -Band Frequency Tripler Using Transformer-Based Self-Mixing Topology With Peaking Inductor. IEEE Transactions on Microwave Theory and Techniques, 2020, 68, 1688-1696.	2.9	12
35	A Wideband CMOS Frequency Quadrupler With Transformer-Based Tail Feedback Loop. IEEE Transactions on Circuits and Systems II: Express Briefs, 2021, 68, 1153-1157.	2.2	12
36	A <i>Ka</i> -Band CMOS Phase-Invariant and Ultralow Gain Error Variable Gain Amplifier With Active Cross-Coupling Neutralization and Asymmetric Capacitor Techniques. IEEE Transactions on Microwave Theory and Techniques, 2022, 70, 85-100.	2.9	12

#	Article	IF	CITATIONS
37	A 220-GHz Compact Equivalent Circuit Model of CMOS Transistors. IEEE Microwave and Wireless Components Letters, 2017, 27, 651-653.	2.0	11
38	A 33.5–39 GHz 5-bit variable gain LNA with 4 dB NF and low phase shift. , 2017, , .		11
39	An Improved RF MOSFET Model Accounting Substrate Coupling Among Terminals. IEEE Microwave and Wireless Components Letters, 2018, 28, 138-140.	2.0	11
40	A 39 GHz MIMO Transceiver Based on Dynamic Multi-Beam Architecture for 5G Communication with 150 Meter Coverage. , 2018, , .		11
41	A Ku-Band 6-Bit Vector-Sum Phase Shifter With Half-Quadrant Control Technique. IEEE Access, 2020, 8, 29311-29318.	2.6	11
42	An Improved Six-Port Equivalent-Circuit Model for Millimeter-Wave On-Chip Transformers With Accurate Coupling Factor Modeling. IEEE Transactions on Microwave Theory and Techniques, 2021, 69, 3989-4000.	2.9	11
43	An Equivalent Circuit Model With Current Return Path Effects for ON-Chip Interconnect up to 80 GHz. IEEE Transactions on Components, Packaging and Manufacturing Technology, 2015, 5, 1320-1330.	1.4	10
44	A 5-Gb/s 66 dB CMOS Variable-Gain Amplifier With Reconfigurable DC-Offset Cancellation for Multi-Standard Applications. IEEE Access, 2018, 6, 54139-54146.	2.6	10
45	Multimode orbital angular momentum antenna based on fourâ€arm planar spiral. Electronics Letters, 2019, 55, 875-876.	0.5	10
46	A 62–85-GHz High Linearity Upconversion Mixer With 18-GHz IF Bandwidth. IEEE Microwave and Wireless Components Letters, 2019, 29, 219-221.	2.0	10
47	Flexible microwave filters on ultra thin Liquid Crystal Polymer substrate. , 2015, , .		9
48	A Wideband Model for On-Chip Interconnects With Different Shielding Structures. IEEE Transactions on Components, Packaging and Manufacturing Technology, 2017, 7, 1702-1712.	1.4	9
49	A Ku-Band 8-Element Phased-Array Transmitter with Built-in-Self-Test Capability. , 2018, , .		9
50	A 22.4-to-40.6-GHz Multi-Ratio Injection-Locked Frequency Multiplier with 57.7-dBc Harmonic Rejection. , 2020, , .		9
51	A SiGe Power Amplifier With Double Gain Peaks Based on the Control of Stationary Points of Impedance Transformation. IEEE Transactions on Microwave Theory and Techniques, 2021, 69, 2279-2290.	2.9	9
52	Support Vector Regression for Measuring Electromagnetic Parameters of Magnetic Thin-Film Materials. IEEE Transactions on Magnetics, 2007, 43, 4071-4075.	1.2	8
53	A <i>K</i> -/ <i>Ka</i> -Band Broadband Low-Noise Amplifier Based on the Multiple Resonant Frequency Technique. IEEE Transactions on Circuits and Systems I: Regular Papers, 2022, 69, 3202-3211.	3.5	8
54	A 24 GHz CMOS mixer using symmetrical design methodology with I/Q imbalance calibration. , 2017, , .		7

#	Article	IF	CITATIONS
55	An Improved Small-Signal Equivalent Circuit Model Considering Channel Current Magnetic Effect. IEEE Microwave and Wireless Components Letters, 2018, 28, 804-806.	2.0	7
56	An improved smallâ€signal equivalent circuit model for 4Hâ€SIC power mesfets. Microwave and Optical Technology Letters, 2008, 50, 1455-1458.	0.9	6
57	Compact multi-band transversal bandpass filters with source–load coupling. Journal of Electromagnetic Waves and Applications, 2014, 28, 184-193.	1.0	6
58	A 27.9–53.5-GHz transformer-based injection-locked frequency divider with 62.9% locking range. , 2017, , .		6
59	RF CMOS Transistor Equivalent Circuit Model up to 66 GHz. , 2018, , .		6
60	An Improved Large Signal Model for 0.1 μm AlGaN/GaN High Electron Mobility Transistors (HEMTs) Process and Its Applications in Practical Monolithic Microwave Integrated Circuit (MMIC) Design in W band. Micromachines, 2018, 9, 396.	1.4	6
61	A Quasi-Physical Large-Signal Statistical Model for 0.15 μm AlGaN/GaN HEMTs Process. , 2019, , .		6
62	A Scalable Model of On-Chip Inductor Including Tunable Dummy Metal Density Factor. IEEE Transactions on Components, Packaging and Manufacturing Technology, 2019, 9, 296-305.	1.4	6
63	A Ka-Band CMOS Variable Gain Amplifier with High Gain Resolution and Low Phase Variation. , 2020, , .		6
64	A Ku-Band Eight-Element Phased-Array Transmitter With Built-in Self-Test Capability in 180-nm CMOS Technology. IEEE Transactions on Very Large Scale Integration (VLSI) Systems, 2022, 30, 694-705.	2.1	6
65	A Ku-band Phased Array in Package Integrating Four 180 nm CMOS Transceivers with On-chip Antennas. , 2018, , .		5
66	An Improved Surface Potential-Based High-Order Channel Length Modulation Model. , 2019, , .		5
67	Multi-bias Small Signal Circuit Model for FinFET Transistors. , 2019, , .		5
68	A 10â€mW 3.9â€dB NF transformerâ€based <i>V</i> â€band lowâ€noise amplifier in 65â€nm CMOS. Internatior Journal of Numerical Modelling: Electronic Networks, Devices and Fields, 2020, 33, e2576.	al 1.2	5
69	An improved wideband equivalent circuit model for integrated spiral inductors in CMOS technology. International Journal of Numerical Modelling: Electronic Networks, Devices and Fields, 2020, 33, e2640.	1.2	5
70	An Improved Surface-Potential-Based Model for MOSFETs Considering the Carrier Gaussian Distribution. IEEE Transactions on Microwave Theory and Techniques, 2020, 68, 4082-4090.	2.9	5
71	An Improved Large-Signal Equivalent Circuit Model for Partially Depleted Silicon-on-Insulator MOSFET. IEEE Transactions on Microwave Theory and Techniques, 2021, 69, 2972-2980.	2.9	5
72	A novel dualâ€band bandpass filter using CRLH triangle mushroom structure and DGS. Microwave and Optical Technology Letters, 2013, 55, 2756-2759.	0.9	4

#	Article	IF	CITATIONS
73	A novel tri-band band-pass filter using combined simplified CRLH and right-handed SIRs. Journal of Electromagnetic Waves and Applications, 2013, 27, 999-1007.	1.0	4
74	CMOS 90 nm multi-bias transistor model Up to 66 GHz. , 2017, , .		4
75	A 27.5â€43.5 GHz 65â€nm CMOS upâ€conversion mixer with 0.42 dBm OP _{1dB} for 5G applications. International Journal of Numerical Modelling: Electronic Networks, Devices and Fields, 2020, 33, e2550.	1.2	4
76	A 68.5~90 GHz High-Gain Power Amplifier With Capacitive Stability Enhancement Technique in 0.13 μm SiGe BiCMOS. IEEE Transactions on Microwave Theory and Techniques, 2020, , 1-1.	2.9	4
77	A Bendable Microwave GaN HEMT on CVD Parylene-C Substrate. , 2020, , .		4
78	An Improved Small Signal Equivalent Circuit Modeling Based On 65nm CMOS Technology. , 2019, , .		3
79	Differential lowâ€loss T/R switch for phase array application in 0.18â€Î¼m CMOS technology. IET Microwaves, Antennas and Propagation, 2019, 13, 813-818.	0.7	3
80	An improved openâ€short equivalent circuit model for CMOS transistors deâ€embedding. International Journal of Numerical Modelling: Electronic Networks, Devices and Fields, 2020, 33, e2589.	1.2	3
81	A millimeterâ€wave scalable small signal model of RF CMOS transistor against number of fingers. International Journal of Numerical Modelling: Electronic Networks, Devices and Fields, 2020, 33, e2608.	1.2	3
82	A 33–41-GHz SiGe-BiCMOS Digital Step Attenuator With Minimized Unit Impedance Variation. IEEE Transactions on Very Large Scale Integration (VLSI) Systems, 2021, 29, 568-579.	2.1	3
83	Complete model for CMOS transistors up to 66GHz. , 2016, , .		2
84	An asynchronous dual switch envelope tracking supply modulator with 86% efficiency. IEICE Electronics Express, 2018, 15, 20180206-20180206.	0.3	2
85	66 GHz biasâ€dependent equivalent circuit model for CMOS transistor based on 90 nanometers CMOS technology. Microwave and Optical Technology Letters, 2018, 60, 1808-1812.	0.9	2
86	A 15-27 GHz Low Conversion Loss and High Isolation Resistive Ring Mixer for Direct Conversion Receiver. , 2019, , .		2
87	A New GSG Pad Compact Model for Skin and Proximity Effect. , 2019, , .		2
88	A Low Noise VCO with Common-Tail Inductor in 180nm CMOS Technology. , 2019, , .		2
89	A high gain CMOS LNA for Ka-Band Communication System. , 2019, , .		2
90	Millimeter wave balun design and optimization based on compensation matching capacitors and active S parameter. International Journal of Numerical Modelling: Electronic Networks, Devices and Fields, 2020, 33, e2644.	1.2	2

#	Article	IF	CITATIONS
91	A Harmonic-Tuned VCO With an Intrinsic-High- <i>Q</i> F ₂₃ Inductor in 65-nm CMOS. IEEE Microwave and Wireless Components Letters, 2020, 30, 981-984.	2.0	2
92	Distributed Characterization of On-Chip Spiral Inductors for Millimeter- Wave Frequencies. , 2020, , .		2
93	Temperature-Dependent Threshold Voltage Extraction of FinFETs Using Noise Measurements. IEEE Transactions on Microwave Theory and Techniques, 2022, 70, 3442-3451.	2.9	2
94	Electromagnetic parameters measurement for thin film materials. , 2008, , .		1
95	Research on microwave properties of CVD graphene by using multiple-layer CPW resonator. , 2012, , .		1
96	Accurate multi-bias equivalent circuit model for graphene resonant channel transistors. , 2016, , .		1
97	A package-level wideband driver amplifier with 134% fractional bandwidth. IEICE Electronics Express, 2018, 15, 20180179-20180179.	0.3	1
98	An Empirical Nonlinear Capacitance Model for SOI Transistor. , 2018, , .		1
99	Single-Fed OAM antenna based on half-mode substrate integrated waveguide. , 2018, , .		1
100	A 2.9 GHz CMOS Phase-Locked Loop with Improved Ring Oscillator. , 2019, , .		1
101	AKa-Band Power Amplifier with 22.9 dBm Psat, 22.5 dBm OP1dB and 21% PAE in 130 nm SiGe BiCMOS. , 2019, , .		1
102	A 5.8 GHz Implicit Class-F VCO in 180-nm CMOS Technology. , 2019, , .		1
103	A High Linearity Low Noise Amplifier for 5G Front-End Modules. , 2019, , .		1
104	A microwave amplifier behavioral model capable of cascade simulation. Microwave and Optical Technology Letters, 2021, 63, 2113-2121.	0.9	1
105	Coupling Effects of Adjacent Inductors on the Transformer in the Millimeter-Wave Regime. , 2021, , .		1
106	An Improved Drain-Current Model for FinFETs. , 2020, , .		1
107	A Complementary Oscillator Using a Current-Limiting Tail Resistor in 180nm CMOS. , 2021, , .		1
108	Detection of Exosomes Using Liquid-Gated Graphene Field Effect Transistor Biosensors. , 2021, , .		1

7

#	Article	IF	CITATIONS
109	The investigation of the signal radiation mechanism of different <scp>GSG</scp> â€pads connection methods. International Journal of Numerical Modelling: Electronic Networks, Devices and Fields, 0, , .	1.2	1
110	Using Support Vector Machine Regression for Measuring Electromagnetic Parameters of Magnetic Materials. , 2007, , .		0
111	Extracting the conductivity of ferromagnetic thin films by using support vector regression. , 2010, , .		0
112	Influence of CPW Dimension on Quality Factor in Microwave Measurement. , 2012, , .		0
113	Design of an X-Band Negative Resistance Oscillator Based on the ASIW in Modern Wireless Communication Systems. , 2014, , .		0
114	A new multipassband filter with multiple transmission zeros based on quarterâ€wavelength resonators in wireless communication systems. Microwave and Optical Technology Letters, 2015, 57, 1105-1107.	0.9	0
115	Single- and multi-layered all-dielectric ENG, MNG, and DNG material parameter extraction by use of the S-parameter method. , 2016, , .		0
116	A K-/Ka-Band 21.4 dBm Power Amplifier with Four-Way Twisted Combiner in \$0.13 mumathrm{m}\$ SiGe BiCMOS. , 2019, , .		0
117	An Improved 220-GHz Small-Signal Equivalent Circuit Model Considering Stray Capacitance Effect. , 2019, , .		0
118	A 2.4 GHz Passive IQ Mixer Using Phase Adjustable Polyphase Filter. , 2019, , .		0
119	A Novel Circularly Polarized Half-Mode/Quarter-Mode SIW Antenna. , 2021, , .		0
120	Model of CPW Transmission Lines with different widths of ground. , 2021, , .		0
121	A 3.65-4.10 GHz Class-C VCO with 189.1 dBc/Hz FoM Based on Low Electromagnetic Coupling. , 2021, , .		0
122	A 3-GHz Inverse-Coupled Current-Reuse VCO Implemented by 1:1 Transformer. IEEE Microwave and Wireless Components Letters, 2022, 32, 434-436.	2.0	0
123	A noise circulating <scp>VCO</scp> with an intrinsic injection locking tripler. International Journal of Numerical Modelling: Electronic Networks, Devices and Fields, 0, , .	1.2	0
124	A Wide-Band Divide-By-2 Injection-Locked Frequency Divider Based on Dual-Resonance Tank. , 2021, , .		0